Canada-US CanSmart Workshop 2001

SMART MATERIALS AND STRUCTURES

Montreal, Quebec, Canada.

FLEXURAL BRAKE MECHANISM FOR INCHWORM ACTUATOR

A. Suleman and S. Burns
suleman@uvic.ca
University of Victoria, Department of Mechanical Engineering
Victoria, B.C., Canada

D. Waechter, R. Blacow and S.E. Prasad
eprasad@uvic.ca
Sensor Technology Ltd.
Collingwood, ON, Canada

ABSTRACT

High force linear actuators today are manufactured on the basis of hydraulic technology. However, there is a strong and increasing demand to switch to a pure solid-state technology, as this would eliminate the flammable and toxic fluids presently used in hydraulic systems. Solid-state devices are more compatible with space applications and can improve the efficiency of the overall system. Presently, most actuators based on solid-state piezoelectric or electrostrictive materials provide either high force with low displacement or low force with high displacement. This paper describes a flexural mechanism that amplifies the displacement of an electrostrictive stack actuator to achieve an intermediate range of both force and displacement.

INTRODUCTION

At present, hydraulic actuators dominate the field of liner actuation. They offer high force and large displacement capabilities. Moreover, they provide variable stroke outputs over a large frequency range. For these reasons, they are the actuator of choice for many aerospace, automotive, and robotic applications. Unfortunately, hydraulic actuators need a separate hydraulic power unit equipped with large electric motors and hydraulic pumps that send the hydraulic fluid to the actuators though hydraulic lines. This supplemental equipment is heavy, expensive, and often requires complicated electrohydraulic interfaces. Furthermore, hydraulic fluids are toxic causing irritation to the skin, eyes, and respiratory tract. The potential danger of this fluid is overwhelming when considering the 40 million cars that are destroyed in the world each year. On average the brake system of each vehicle contains ≈ 0.7l of hydraulic fluid.

Assuming that only ~ 70% is recoverable, ≈ 8,000 tons is emitted into the environment in an unknown way. The brake fluids contain oligoglycol ethers, which are carcinogenic or can promote genetic damages and corrosion inhibitors, like benzotriazols or tolyltriazols. Furthermore, hydraulic fluids are flammable.

Strain-Induced Actuators

The basic motivation is to replace the hydraulic actuators that use polluting fluids and require heavy and expensive supplemental equipment. Solid-state induced strain actuators offer a promising alternative. Typically solid-state induced strain actuators can generate high forces albeit low displacements. Nevertheless, by means of the inchworm concept, strain induced actuators can deliver high displacements as well as high forces. Thus, in many applications, replacing existing hydraulic with strain-induced actuators is a viable alternative. Another motivation for the advancement of strain-induced actuators is driven by their use in the space industry. An example is the use of electrostrictive actuators used for the correction of the aberrations in the Hubble Telescope. An adaptive structure can adopt a wide range of geometric configurations by lengthening or shortening some of its active elements. This ability allows these structures to adopt special configurations in order to maximize the structural strength. This technology has proved helpful in many space truss systems including large span roof trusses, space reflectors, and robotic arms. Other uses including: release mechanisms, positioning devices, vibration suppression, dexterity and obstacle avoidance.

The uses for strain-induced actuators are not limited to space applications. In fact strain-induced actuators have many earth bound uses as well. Some of these include: micro-positioning xy-tables, ultrasonic motors, impact printer heads, vehicle suspensions, and precision machining. With such a vast number of applications the demand to further advance induced-strain actuator technology is obvious.

Previous Inchworm Actuator Designs

During the past 40 years, piezoceramic inchworm actuator designs have been proposed based on two or more piezoceramic stacks for griping and extension, as illustrated in Fig. 1. In 1964, Stibitz and Steele used a magnetostrictive material on the end of three rods. Each of the three rods would grip, release or push the inner shaft in a predetermined sequence that would actuate the shaft. McNancy (1996) developed an amplification device consisting of a piezoceramic stack that was specially positioned against ball bearings. The displacement of the piezoceramic was transferred and amplified though the ball bearings.

Next, a hollow cylinder design with an inner clamping and extending device was proposed (Hsu, 1966). Locher (1967) developed a mechanism that used two cams to grip and release an inner shaft. The inner shaft contained a piezoceramic material producing the extension. Other contributions include the works by Next, Brisbane (1968) invented an inchworm actuator using a tube and an inner crawler. The crawler had three piezoceramic elements: two for gripping and one for extension. In 1972, Galutva designed an actuator, which consisted of several piezoceramic elements used for gripping and extending. In 1975, Bizzigotti and May introduced an inchworm actuator that used curved surfaces to grip the outside of a shaft. The piezoceramic on one end would grip the shaft while the center piezoceramic would extend. After extension, the piezoceramic on the other end would grip the shaft to capture the

displacement. In 1976, Sakitani invented the inchworm actuator that would clap and extend on a surface providing a precise displacement. In 1979, Ishikawa developed an actuator similar to the design of Bizzigotti but incorporated the use of two extending piezoceramic elements instead of one. In 1980, O'Neill reported the first stacked piezoceramic actuator. The idea of stacking increased the actuator displacement. The design involved a cylindrical tube with an inside crawler. In 1984, Taniguchi presented an actuator that used an outer cylindrical shell and an inner crawler. The inner crawler consisted of several cylindrical piezoceramic elements stacked together. The actuation technique made the inside crawler creep inside the outer shell more like an earthworm than an inchworm.

In 1986, Hara modified the design of Bizzigotti and May by incorporating stacked piezoceramics to increase the actuation displacement. In 1986, Staufenberg created an actuator capable of transnational and rotational motion. Many piezoceramics were used in the design. Some were used grip the shaft were others were used to push the shaft outward (translational motion) or to push the shaft sideways (rotational motion). In 1987, Fujimoto positioned piezoceramics on the outside of a disk producing a rotational motion. In 1990, Murata used one set of piezoceramics to engage a shaft with an extremely small pitch. Once engaged, the shaft would be actuated by another set of piezoceramics. In 1994, Rennex used piezoceramics with flexure clamps to hold and actuate the inner shaft. In 1994, Miesner and Teter developed a piezoceramic actuator that used piezoceramics on the ends for clamping and in the center for extension. In 1996, Pandell and Garcia designed an actuator similar to the design of Galutva but having one extra stage for extension and clamping. More recently, Galante (1997) designed an actuator having an inner shaft that moves with respect to the outer casing. The inner shaft has one piezoceramic used for extension, whereas the outer casing had two piezoceramics used for gripping. Actuating the piezoceramics in a special sequence forced the inner shaft to move. All the reported designs have resulted in either a high displacement/low force or in a low displacement/high force capability. The objective of the proposed inchworm actuator is to obtain a moderate force/moderate displacement actuator for space applications.

Design Specifications

The design considerations consist of the actuator specifications and the material selection. The actuator is required to meet the specifications presented in Table 1.

Table 1 Actuator Design Specifications

Maximum Displacement (microns)	**15,000**
Maximum Force (N)	**20 - 30**
Maximum Bandwidth (Hz)	**5,000**
Maximum Operating Voltage (V)	**300**
Minimum Operating Temperature (C)	**-100**
Maximum Operating Temperature (C)	**100**
Hysteresis (%)	**3 - 12**
Capacitance (nF)	**100 - 250**

Actuation Materials

The selected actuation material must provide adequate elongation when an electric field is applied. Therefore, electromechanical ceramics are an understandable choice as their

dimensions change as a result of an applied electric field. Piezoceramics are field-induced materials that can be broken down into two categories. The first category is made from lead zirconate titanate (PZT), which exhibits piezoelectric properties. The second is lead magnesium niobate (PMN), which exhibits electrostrictive properties. Piezoelectric materials have been used as transducers for sensing and generating small pressure perturbations associated with acoustic waves in both air and water. Today, piezoelectric materials are used in a variety of applications including actuators, optics (laser cameras), precision machinery, motors, buzzers, transformers, and sensors. These applications are possible due to the material's special electrical and mechanical coupled properties known as the piezoelectric effect. When an electric field is applied to a piezoelectric crystal it expands. Conversely, when the field is reversed the crystal contracts. This is known as the inverse piezoelectric effect and is most useful for actuator applications. Electrostrictive materials exhibit field-induced strains where the material strain is proportional to the square of electric field. Electrostrictive materials expand regardless of the polarity of the electric field and exhibit negligible hysteresis at low fields.

ACTUATOR DESIGN AND MODELLING

The inchworm actuator concept uses small incremental steps to attain large displacements. This motion is achieved by a mechanism that "walks" inside an outer casing. The walking mechanism consists of two brake assemblies separated by a center piezoceramic stack, as shown in Fig. 2. Each brake assembly is forced to clap and unclamp in a particular sequence to capture the displacement of the center stack. Consequently, the brake assemblies are the most critical aspect of the actuator design (Fig. 3).

The metal for the flextensional frame and the outer casing was chosen to be the same to eliminate any variation in thermal expansion between two dissimilar metals. The metals that were investigated include aluminum, stainless steel, brass and titanium. The metal of choice must have a high Young's modulus to efficiently transfer the stack displacement to the brake pads and must have a coefficient of thermal expansion similar to the chosen piezoceramic. Based on the Young's modulus alone Stainless Steel 304 and Titanium (6% Al, 4%V) are likely choices. However, since the coefficient of thermal expansion for the chosen piezoceramic is ~3 E-6/^{0}C, Titanium (6% Al, 4% V) having at thermal coefficient of 9.5 E-6/^{0}C is therefore the best choice. Moreover, Titanium (6% Al, 4%V) has a high strength to weight ratio (density = 4730 Kg/m^3), which makes it even more advantageous for space applications.

Firing each stack in a predetermined sequence creates the actuator motion. First, the top stack is energized releasing the top brake pads. Next, the center stack is actuated pushing the top brake assembly upward. Afterward, the top stack is de-energized forcing the top brake pads to grip the outer casing. Next, the bottom stack is fired releasing the bottom pads. Subsequently, the center stack is de-energized moving the bottom brake assembly up. Finally, the bottom stack is de-energized forcing the bottom pads to grip the outer casing and capture the displacement. This sequence is repeated in rapid succession emulating the movement of an inchworm.

When the piezoceramic stack is energized the surrounding material (flextensional frame) is

forced to flex and change dimension. The flextensional frames are designed to have an interference fit with the outer casing. When energizing the brake stacks the frames are forced to distort reducing their width. This action frees the flextensional frames and allows them to move freely within the outer casing. When the stacks are de-energized the frames grip the outer casing locking the actuator in place.

The actuator design incorporates circular notches in the flextensional frames to facilitate bending at targeted locations. Additionally, a rod with adjusting nuts has been inserted through the center of the actuator. In this design, each brake assembly incorporates two pre-stressing adjustments: one for the stack, and one for the frame. When adjustment, the nuts are tightened so that the stack is pre-stressed. This ensures the stacks always remain in compression. When adjustment nuts 1 and 3 are tightened the frame is pre-stressed. Pre-stressing the frame allows a fine width adjustment within the outer casing. This design has the advantage of maintaining a locked position when no electrical power is supplied. Moreover, the design has few parts and is adjustable.

Finite Element Model

The actuator design has been modeled using the finite element software ANSYS. The stack was modeled using the 10-node tetrahedral element type. This element is defined by ten nodes with up to six degrees of freedom at each node. The stack is assembled from "wafers" of piezoelectric or electrostrictive material each having a thickness of 0.254mm (0.01in) with an outer diameter of 25.4mm (1in) and an inner diameter of 6.35mm (0.25in). The stack contains 200 wafers stacked and glued together with an adhesive material achieving a total height of 57.15mm (50.8mm from the wafers and 6.35mm from the adhesive). The stack model contains 5,978 nodes, 3,645 elements and has 22,488 active degrees of freedom.

Consider first the stack make from the piezoelectric material. When one end was fixed and 200V was applied across each wafer the stack elongated a free displacement of 6.8um. When both ends were fixed and each wafer was subject to 200V a blocked force of 3,192N was measured. Next, consider an identical stack made from the electrostrictive material. When fixing one end and applying 200V across each wafer, the stack moved a free displacement of 36.0um. Next, fixing both stack ends and applying the same voltage a blocked force of 29,924N was measured. Comparing the performance of the two ceramics it is apparent that the electrostrictive material is significantly superior then the PZT in both the free displacement and blocked force criteria. The electrostrictive has therefore been selected as the actuation material.

Table 2 Comparison of the Free Displacement and Blocked Force of PZT and PMN

	PZT		PMN	
	Ansys	**Exp.**	**Ansys**	**Exp.**
Free Disp. (μm)	6.8	7.3	36.0	36.0
Blocked Force (N)	3192	3592	29924	33661

Brake Assembly Modeling

The flextensional frame was created using the solid element. The brake assembly model is shown in Fig. 4 The model contains12,455 nodes, 6,512 elements and 38,063 dof.

Brake Assembly Design Parameters

The design parameters were classified as the fixed and the free parameters (Fig. 3):

Fixed Parameters. The fixed dimensions were set due to the size and shape of the PMN stacks. These stacks have an outer diameter of 25.4mm (1in), an inner diameter of 6.35mm (0.25in), and height of 57.15mm. The minimum clearance required to adjust nut 2 was 10mm. Therefore 10mm was chosen. The recommended pre-stress on the PMN stack was 2400N (or 733psi). The last fixed dimension was the threaded rod diameter. It was chosen to be 0.1875in as it was the next nominal size smaller than the PMN stack hole of 0.25in.

Free Parameters. Instead of simultaneously trying to fix all the dimensions in the Ansys model, one at a time was varied and selected. The dimensions having the greatest impact on the design were selected first and these include the notch thickness, shoulder thickness; arm thickness; arm angle; notch diameter; and casing pre-stress.

Performance Criteria

To assist in the selection of the free dimensions three performance variables were defined; namely: the actuation range, the blocked force, and the fatigue safety factor.

Range: The range is important because it is a measure of the brake pad movement during actuation. Too small a range may not allow the brake pad to free itself from the outer casing.

Blocked force. For the brake pad to come in and out of contact, the outer casing must be located somewhere between the maximum and minimum brake pad lateral displacements. To ensure the brake pads release from the outer casing during actuation there should be a clearance. The minimum suggested clearance is 25.4um (0.001in). To make certain the pad release, the design aims for a clearance between 25.4um (0.001in) and 50.8um (0.002in).

Fatigue safety factor. The operation of this actuator requires the flextensional frame to bend back and forth a high number of cycles. Each cycle induces a fluctuating stress, which over time may results in the possibility of fatigue failure. To safeguard against this, a fatigue analysis was preformed for each potential design. Using the Modified Goodman relation, along with the surface roughness taken as machined, the allowable stress amplitude was calculated for each design. Subsequently, the actual stress amplitude was also determined for each design. Dividing the allowable stress amplitude by the actual stress amplitude gives the Fatigue Safety Factor. Investigating the possible locations for fatigue failure it was determined that the most critical location was at the center notches.

Final Design

The final design free dimensions are: notch thickness = 1mm; shoulder thickness = 9mm; arm thickness = 5mm; arm angle = 4.87°; notch diameter = 2.5mm; and casing pre-stress = 567N. Some of the finite element simulation results are shown in Figs. 5, 6 and 7.This final design produced the theoretical results shown in Table 3.

Table 3 Final Design Results

Brake	Disp.	Blocked

Pad Clearance (μm)	Range (μm)	Force (N)
0	106	86
25.4	106	64
50.8	106	42
76.2	106	19

EXPERIMENTAL PROTOTYPE

The inchworm experimental device was set up as shown in Fig. 8. An LVDT was used to measure displacement at any one of the four positions shown. Because there was only one LVDT the measurements could not be done simultaneously. Tests were performed at a given position, then the LVDT was moved to the next position and the measurements were repeated. Two weights, one 685 g and the other 2156 g were used to check the braking forces. It was found that the inchworm device as currently adjusted had insufficient braking force on the two brakes (0 V on both) to support the 2156 g weight.

The inchworm device was operated without additional weight and with a 2 s period and with step voltages on each actuator of 300 V. LVDT and control signal data were recorded for each of the four positions for a total of 5 periods. Fig. 8 also shows the results for the second and third periods are shown. The scale has units of microns so that the actual spatial steps can be measured from the graphs. However the positions of the LVDT curves were vertically shifted relative to each other for display purposes. The signal curves do not show actual voltages but are placed on the same scale to show the timing. Table 3 shows the total displacement over two periods, which should in principle be position independent. But because the results are measured over different cycles there are noticeable differences. The downward displacement is ~ 20 microns per cycle. This is actually a bit more than expected (stack displacement at 300 V was measured as ~ 16 microns), which suggests that there was slippage. To check that the brakes were balanced and had the required forces for correct operation, the following tests were performed. In the first test zero additional weight was placed on the device and applying 300 V to the upper brake stack removed the upper braking force. Then the voltage on the lower brake stack was increased from zero in 10 V steps at a rate of 10 V every 2 s. The voltage when the inchworm device fell under its own weight was recorded. This occurred at 200 V. In the next test, 300 V was applied to the lower brake and the upper brake voltage was increased from zero in the same manner until the device fell under its own weight. This also occurred at 200V, thus showing that the two brake forces was approximately balanced. In the next test, a 685 g weight was placed on the top of the actuator and both brake voltages were initially set to zero. The two brakes together were sufficient to hold this weight. Then the voltage on only one brake was raised in the same manner as before and the voltage when the weight dropped was recorded. For both brakes this occurred at 170 V. This again shows that the brakes are approximately balanced, but also shows that one brake alone is insufficient to hold 685 g. At the present time, there is a new prototype being built made totally of titanium machined using a high precision EDM method. Further tests are being carried out to quantify the performance of the actuator.

CONCLUDING REMARKS

A new flexural mechanism that amplifies the displacement of an electrostrictive stack actuator to achieve an intermediate range of both force and displacement has been designed and partially tested. The finite element model simulation results have provided the final design parameters and further tests are underway to quantify the performance of the actuator.

REFERENCES

Bizzigotti, R. A., "Electromechanical translational apparatus". *US. Patent: 3,902,085,* 1975.

Brisbane, A.D., "Position control device", *U.S. Patent: 3,377,489,* 1968.

Fujimoto, T., "Piezo-electric actuator and stepping device using same", *US Patent: 4,714,855,* 1987

Hara, A., H. Takao, Y. Kunio, and N. Keiji, "Electromechanical translation device comprising an electrostrictive drive of a stacked ceramic capacitor type", *US Patent: 4,570,096,* 1986.

Hsu, K., and A. Biatter, "Transducer", *U.S. Patent: 3,292,019,* 1966.

Ishikawa, and Y. Sakitani, "Two-directional piezoelectric driven fine adjustment device", *U.S. Patent: 4,163,168,* 1979

Locher, G.L, "Micrometric linear actuator", *U.S. Patent: 3,296,467,* 1967.

Meisner, J.E. and . Teter , J.P, "Piezoelectric/magnetostrictive resonant inchworm motor", *SPIE*, Vol. 2190, pp. 520-527, 1994.

Murata, T., "Drive apparatus and motor unit using the same", *U.S. Patent: 4,974,077,* 1990.

O'Neill, G., "Electromotive actuator", *U.S. Patent: 4,219,755,* 1980.

Pandel, T. and Garcia E., "Design of a piezoelectric caterpillar motor" *Proceedings of the ASME aerospace division*, AD-Vol. 52, pp. 627-648, 1996.

Rennex, "Inchworin actuator", *U.S. Patent: 5,3323,942,* 1994.

Sakitani, Y., "Stepwise fine adjustment", *U.S. Patent: 3,952,215,* 1976.

Staufenberg, C.W., Jr., and R.J. Hubbell, "Piezoelectric electromechanical translation apparatus", *U.S. Patent: 4,622,483,* 1986.

Stibitz, R., "Incremental Feed Mechanisms", *U.S. Patent: 3,138,749,* 1964..

Taniguchi, T., "Piezoelectric driving apparatus", *US Patent: 4,454,441,* 1984.

	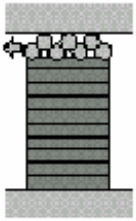	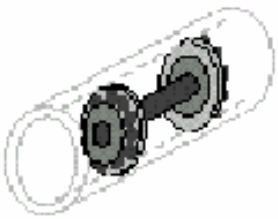
Stibitz, 1964	McNancy, 1964	Hsu, 1966

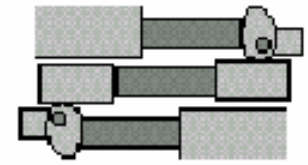	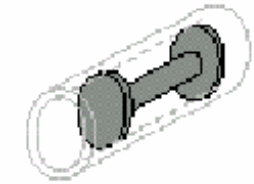	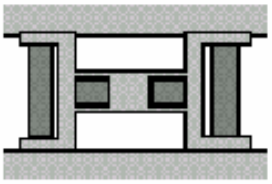
Locher, 1967	Galutva, 1972	Brisbane, 1968
	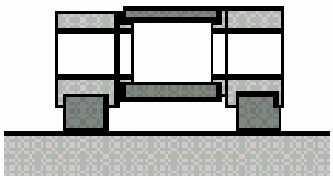	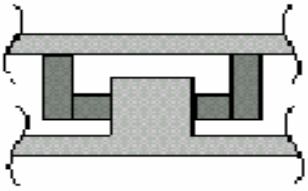
Bizzigotti and May, 1975	Sakitani, 1976	Ishikawa, 1979
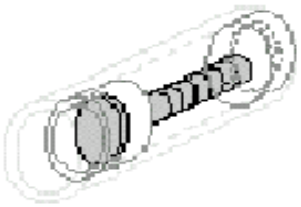	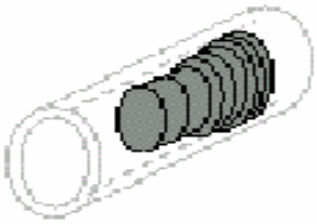	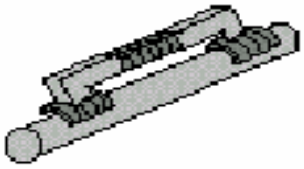
O'Neill, 1980	Tanigushi, 1984	Hara, 1986
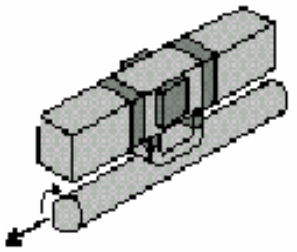	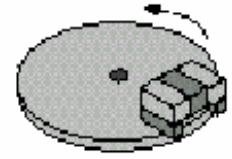	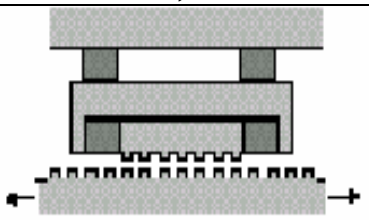
Staufenberg, 1986	Fujimoto, 1987	Murata, 1990
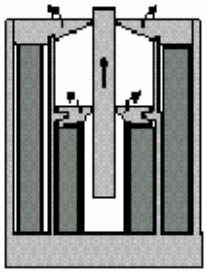		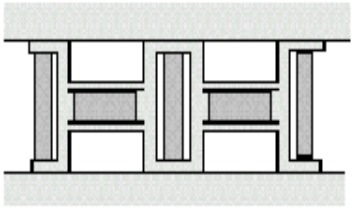
Rennex, 1994	Miesner and Teter, 1994	Pandell and Garcia, 1996

Figure 1 – Inchworm actuator designs reported in the literature

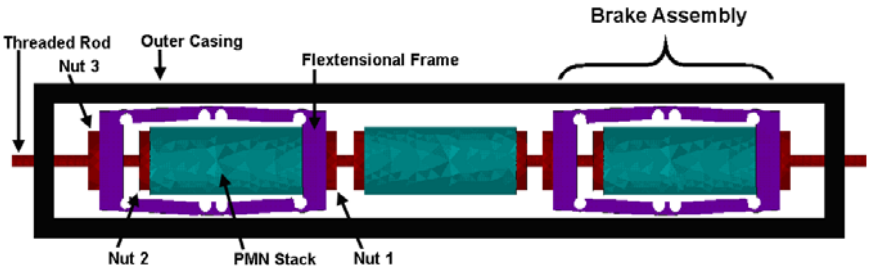

Figure 2 – Proposed inchworm actuator

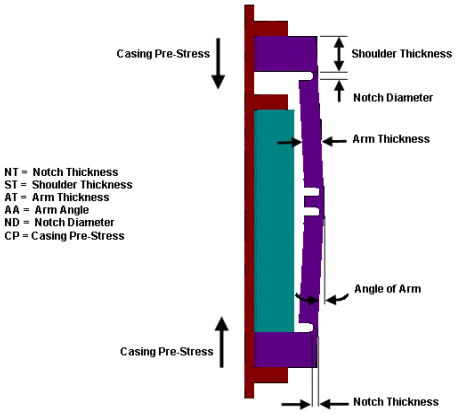

Figure 3 – Design parameters

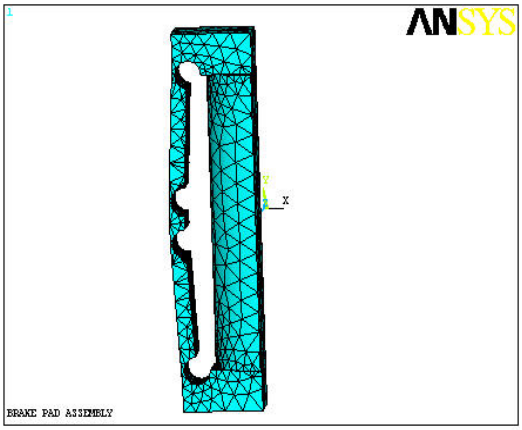

Figure 4 – FE model of brake and stack

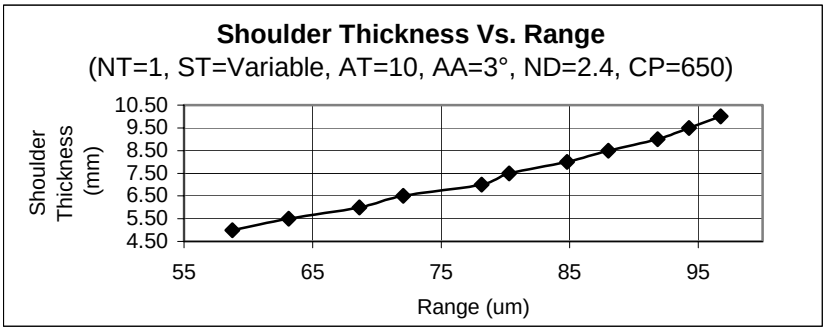

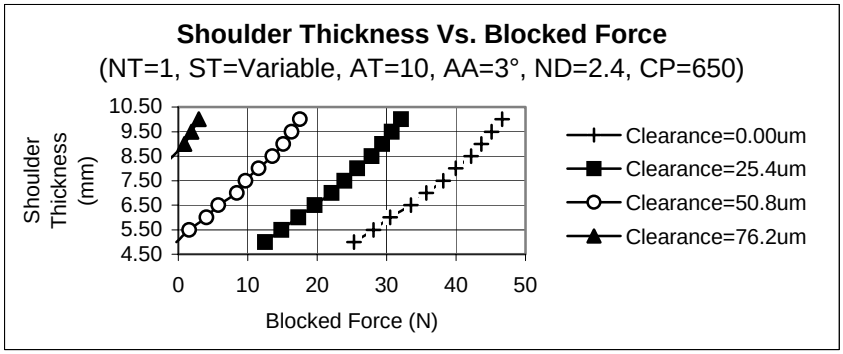

Figure 5 – (a) Shoulder thickness vs. range; and (b) shoulder thickness vs. blocked force

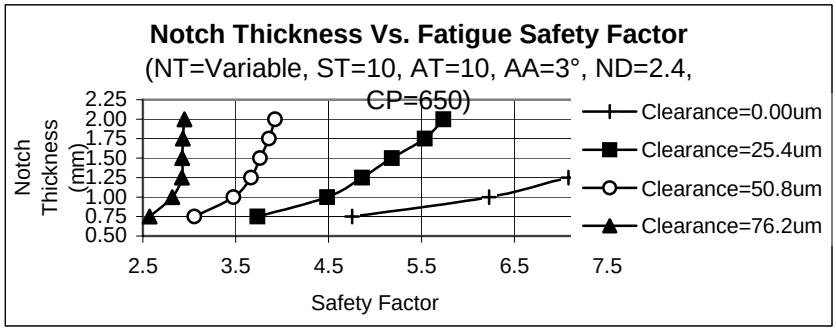

(a)

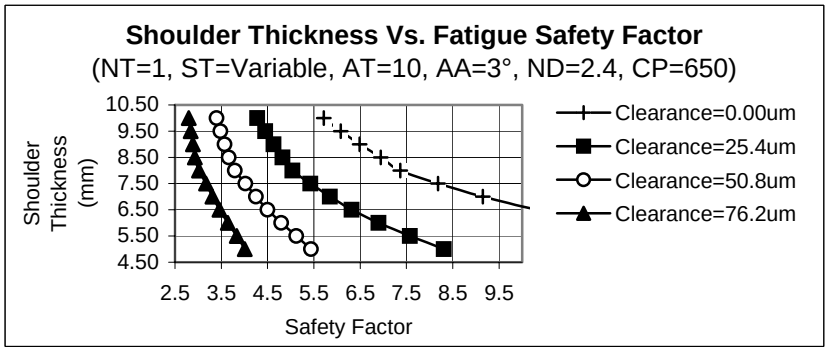

(b)

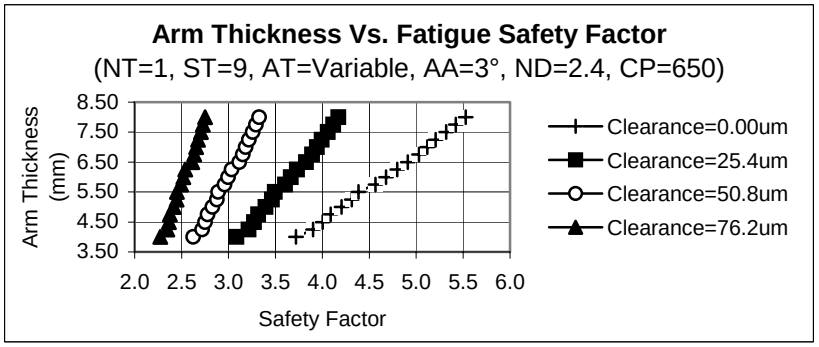

(c)

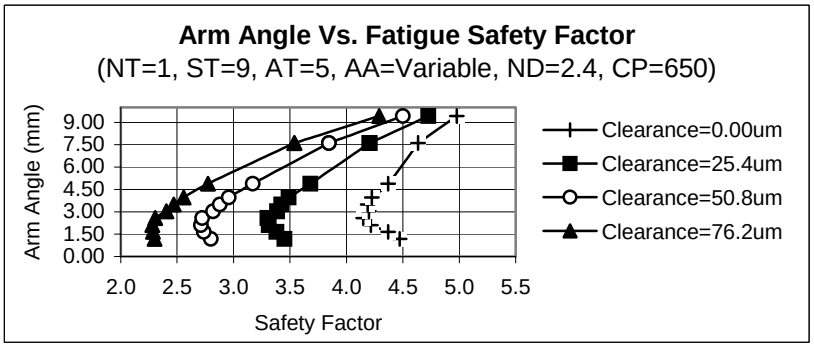

(d)

Figure 6 – Design parameters versus fatigue safety factor

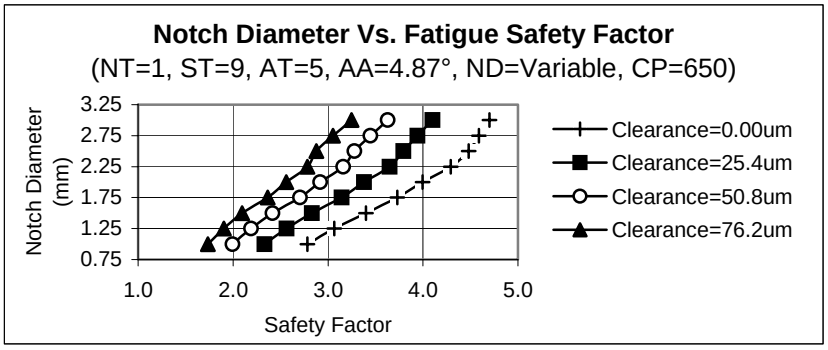

(a)

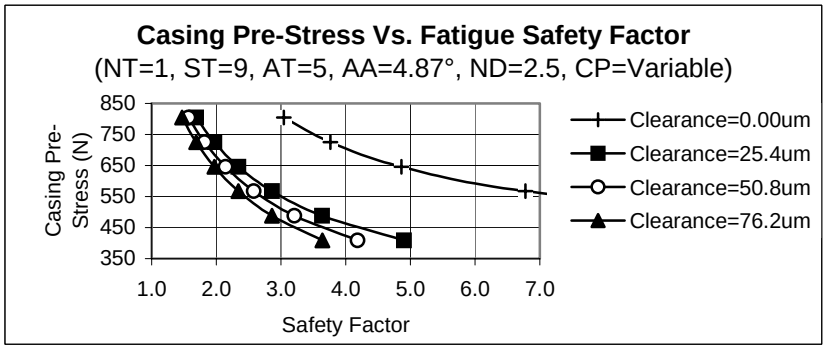

(b)

Figure 7 - Design parameters versus fatigue safety factor

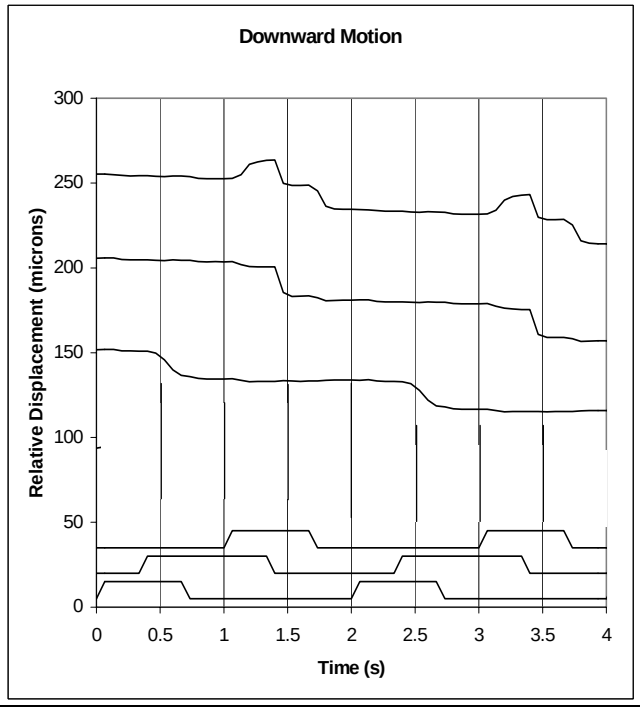

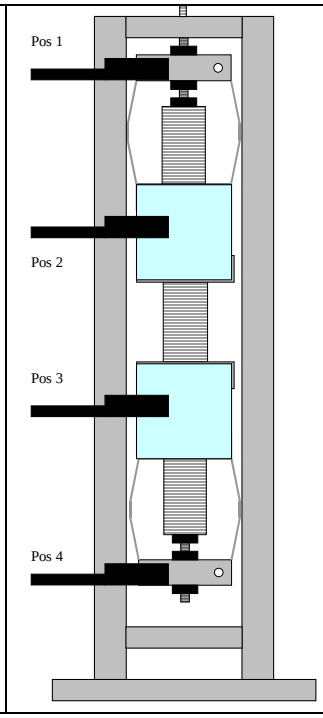

Figure 8 - Experimental displacement and timing curves. Moving from the top curve to the bottom curve, the curves are the displacement signals for Pos 1, 2 & 3, and the electrical signals (arbitrary units) for the upper brake, extender and lower brake.